SZENT ISTVÁN UNIVERSITY
GÖDÖLLŐ

Numerical modelling of material properties of textile composite

Thesis of PhD work

Gergely Bojtár

Gödöllő, Hungary
2019

Doctoral school denomination: Mechanical Engineering PhD School

Science: Agricultural Engineering

Leader: Prof. Dr. István Farkas
Full Professor, DSc
Faculty of Mechanical Engineering
Szent István University, Gödöllő, Hungary

Supervisors: Dr. Béla M. Csizmadia †
Professor Emeritus, CSc
Institute of Mechanics and Machinery
Faculty of Mechanical Engineering
Szent István University, Gödöllő, Hungary

Prof. Dr. János Égert
Full Professor, CSc
Faculty of Mechanical Engineering,
Information Technology and Electrical Engineering,
Department of Applied Mechanics
Széchenyi István University, Győr, Hungary

....

Affirmation of head of school Affirmation of supervisor

CONTENTS

LIST OF SYMBOLS, ABBREVIATIONS

u, v, w	scalar coordinates of the displacement vector
E_1, E_2, ν_{12}, G_{12}	planar orthotropic material constants of the composite layer
E_{r1}, E_{r2}, E_{r3}	Young's moduli of the roving
ν_{r12}, ν_{r23}, ν_{r13}	Poisson's ratios of the roving
G_{r12}, G_{r23}, G_{r13}	shear moduli of the roving
E_{f1}, E_{f2}, E_{f3}	Young's moduli of the reinforcing fiber
ν_{f12}, ν_{f23}, ν_{f13}	Poisson's ratios of the reinforcing fiber
G_{f12}, G_{f23}, G_{f13}	shear moduli of the reinforcing fiber
E_m, ν_m, G_m	isotropic material constants of the matrix
$\bar{\sigma}_1$, $\bar{\sigma}_2$, $\bar{\tau}_{12}$	homogenized/average stress coordinates in the composite layer
$\bar{\varepsilon}_1$, $\bar{\varepsilon}_2$, $\bar{\gamma}_{12}$	homogenized/average strain coordinates in the composite layer
$\bar{\sigma}_{r1}$, $\bar{\sigma}_{r2}$, $\bar{\sigma}_{r3}$	homogenized/average normal stresses in the roving
$\bar{\tau}_{r12}$, $\bar{\tau}_{r23}$, $\bar{\tau}_{r13}$	homogenized/average shear stresses in the roving
$\bar{\varepsilon}_{r1}$, $\bar{\varepsilon}_{r2}$, $\bar{\varepsilon}_{r3}$	homogenized/average normal strains in the roving
$\bar{\gamma}_{r12}$, $\bar{\gamma}_{r23}$, $\bar{\gamma}_{r13}$	homogenized/average shear strains in the roving
F_i	resultant reaction force in the direction x_i on the side face of the layer model cell
F_{ri}	resultant reaction force in the direction x_{ri} on the side face of the roving model cell
n_1, n_2	density of rovings in the directions x_1 and x_2 in the textile
t_1, t_2	distance of rovings in the directions x_1 and x_2 in the textile
λ	ratio of longitudinal to transverse rovings in the textile
φ_f	ratio of volume of the reinforcing fibers to the volume of the textile in the composite layer

1. INTRODUCTION AND OBJECTIVES

Textile composites and objectives of the thesis are presented in this chapter.

1.1. Introduction

Composite materials are materials with heterogeneous structure and are made up of a combination of two or more different materials. Mainly layered fiber-reinforced plastics are used in (mechanical) engineering practice.

Layered textile composite structures generally comprise fiber reinforcement in the form of a fabric in each layers. A planar, two-dimensional (2D) fabric is a textile which has a small thickness compared to the other two dimensions. Thousands of elementary fibers are arranged in roving in the fabric. The rovings can be untwisted or twisted. During production matrix material is also introduced into the rovings (among the elementary fibers). Such a heterogeneous material structure is shown in Fig. 1. The heterogeneous material structure can be treated with a macroscopic material model, which is not suitable for the determination of stresses and strains in the fibers and the matrix, only the homogenized mechanical properties of a smaller range can be determined.

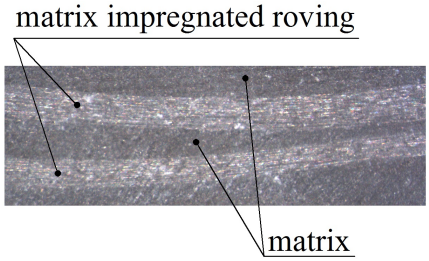

Fig. 1. Heterogeneous structure of a composite

1.2. Objectives

The mechanical design of composite machine structures requires the macroscopic material properties of each composite layer. The studied structure is modeled with layered composite shell elements in finite element programs. Homogenized orthotropic material constants of these layers E_1, E_2, ν_{12}, G_{12} in the principal coordinate system, thickness of the layers, orientation angle of the principal axis x_1 have to be given as input data. The aim of this dissertation is to develop and modify finite element models developed for the determination of macroscopic material constants of the composites described in the literature in order to make the material constants produced by them more accurate. A further aim is to investigate how the

structure and material properties of the reinforcing textile influence the macroscopic material properties of the composite layer. It is one of the most important issues in material design. I set out the following tasks in my dissertation:

1. Development and construction of a finite element model cell of a roving embedded in a composite matrix. Performing a finite element analysis with a roving model cell for tension in all three principal directions and for pure shear in all three planes. Numerical determination of the macroscopic orthotropic material properties of the roving from the results of the finite element modeling after providing appropriate boundary conditions.
2. Development and construction of a finite element model cell for modeling a layer of a textile composite sheet. Providing proper boundary conditions for tension in the plane of the layer in both principal directions and for pure shear. Numerical determination of planar macroscopic orthotropic material properties of the composite layer by finite element modeling of the layer model cell.
3. Checking the applicability of finite element model cells and clarifying the necessary finite element modeling conditions for the use of developed numerical methods.
4. Production and experimental investigation of multilayer (with the same fiber arrangement in each layer), tensile and shear composite specimens of a given textile and matrix material to determine the macroscopic material properties of a textile composite layer. Comparison of measurement results and numerical results of finite element modeling, thereby validating the finite element roving model cell and textile composite layer.
5. Numerical studies with finite element model cells to clarify how the parameters of design of the composite change the orthotropic material properties of a textile composite layer.
   Cases studied:
   a) Effect of Young's modulus of reinforcing fibers on the macroscopic material properties of the layer.
   b) Effect of the type of weaving of the textile on the macroscopic material properties of the composite layer.
   c) Dependence of the material properties of the layer on the volume ratio of the textile.
   d) Dependence of the material properties of the layer on the ratio of longitudinal to transverse rovings.

2. MATERIAL AND METHOD

Textile composite layer used in experiments and modeling will be presented in this chapter. Finite element model cells of roving and finite element model cells of textile composite layer will be constructed. Procedure of determination of homogenized, orthotropic material properties will be described.

2.1. Textile composite layer used in experiments and modeling

Two eight-layer textile composite sheets were laminated manually, one of which is shown in Fig. 2. Specimens were cut out from them. The orthotropic material properties determined by experiments of the eight-layer textile composite sheet are in good agreement with those of a single layer of the sheet. In the thesis a layer of the textile composite sheet shown in Fig. 2 is modeled with a layer model cell.

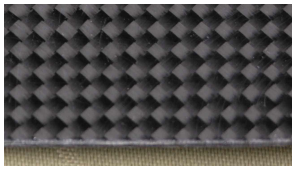

Fig. 2. Top view of textile composite sheet

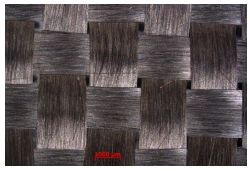

Fig. 3. Plain weave fabric

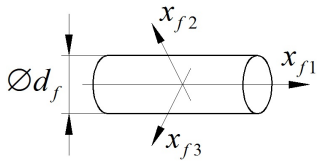

Fig. 4. Coordinate system $x_{f1}x_{f2}x_{f3}$

Table 1. Material constants of a carbon fiber and polyester resin

Carbon fiber		Poliester resin
$E_{f1} = 230\,000$ MPa	$E_{f2} = E_{f3} = 15\,000$ MPa	$E_m = 3\,677$ MPa
$\nu_{f12} = \nu_{f13} = 0{,}166$	$\nu_{f23} = 0{,}400$	$\nu_m = 0{,}346$
$G_{f12} = G_{f13} = 6\,432$ MPa	$G_{f23} = 5\,357$ MPa	$G_m = 1365{,}9$ MPa

Each layer of the composite sheet is reinforced by plane weave carbon fabric with type SIGRATEX KDL 8003. Carbon fabric used is shown before impregnation in Fig. 3. Elementary carbon fibers of diameter $d_f = 7$ μm are arranged in flat, untwisted rovings. The type of the roving is Torayca T300-3K in directions of warp and weft. There are $n_f = 3\,000$ carbon fibers in a roving. Table 1 shows the orthotropic material constants of a carbon fiber of a roving in the coordinate system of the principal axes $x_{f1}x_{f2}x_{f3}$ shown in Fig. 4. The carbon fiber is isotropic in transverse direction, shear modulus G_{f23} can be determined by formula (45). The matrix is poliester resin with type AROPOL M105TB. It is homogeneous, linear elastic, isotropic. Its

material properties were determined by measurements (Table 1).

2.2. Finite element roving model cells

The composite layer contains textile weaved from rovings which is embedded in matrix material. The rovings contain thousands of reinforcing fibers which are also impregnated by matrix material.

Finite element model cell of a roving is shown in Fig. 5. It is the repeting domain of the composite roving which builds up the whole roving. μm is chosen for length unit of the roving model cell and unit system (kg, μm, s, μN, MPa) is used. The figure also identifies the six sides of the cell. Characteristic geometric data of the roving model cell of the textile composite sheet studied are as follows:

$d_f = 7\ \mu\text{m}$, $a = 7{,}613\ \mu\text{m}$, $b = 13{,}186\ \mu\text{m}$,

$A_{A+} = A_{A-} = A_{B+} = A_{B-} = 100{,}385\ \mu\text{m}^2$, $A_{C+} = A_{C-} = 57{,}958\ \mu\text{m}^2$.

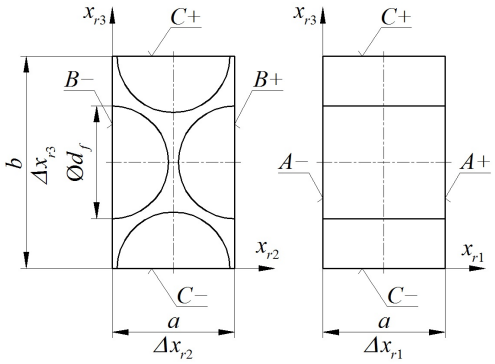

Fig. 5. Dimensions of model cell of a roving

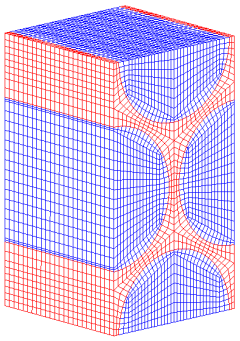

Fig. 6. Finite element mesh of model cell of a roving

Finite element mesh of roving model cell is shown in Fig. 6. The nodes on the opposite surfaces are at the same plane coordinates, and so pairs of nodes are created in the model cell.

Due to the symmetry of the model cell, the macroscopic material properties are the same in directions x_{r2}, x_{r3} and in planes $x_{r1}x_{r2}$, $x_{r1}x_{r3}$. Therefore the roving has only 6 independent orthotropic material constants:

$$E_{r1}, \quad E_{r2} = E_{r3}, \quad \nu_{r12} = \nu_{r13}, \quad \nu_{r23}, \quad G_{r12} = G_{r13}, \quad G_{r23}.$$

If the elementary fibers are orthotropic but transversely isotropic, the matrix impregnated roving will also have this property due to the hexagonal arrangement of fibers. Shear modulus G_{r23} can be determined by relation valid for isotropic case:

$$G_{r23} = \frac{E_{r2}}{2\left(1+\nu_{r23}\right)}. \tag{1}$$

Material constants determinable in the given load case are shown in Table 2. All the 6 load cases were investigated. It was even a check for relations between the material properties. Finite element modeling of tension in the direction x_{r1} is presented in the booklet of thesis.

Table 2. Characteristic material constants of a roving

Simulated load cases	Determinable material constants	Check
Tension in direction x_{r1}	E_{r1}, ν_{r12}, ν_{r13}	$\frac{\nu_{rij}}{E_{ri}} = \frac{\nu_{rji}}{E_{rj}}$ $\nu_{rji} = \frac{E_{rj}}{E_{ri}}\nu_{rij}$ $(i \neq j = 1,2,3)$
Tension in direction x_{r2}	E_{r2}, ν_{r21}, ν_{r23}	
Tension in direction x_{r3}	E_{r3}, ν_{r31}, ν_{r32}	
Shear in plane $x_{r1}x_{r2}$	G_{r12}	
Shear in plane $x_{r2}x_{r3}$	G_{r23}	
Shear in plane $x_{r1}x_{r3}$	G_{r13}	

In order to ensure repetition, *kinematic load* (a nodal displacement field) is specified for the roving model cell. Numbers shown in Fig. 7 refer to the nodes in the vertices and at the center of the sides of the model cell.

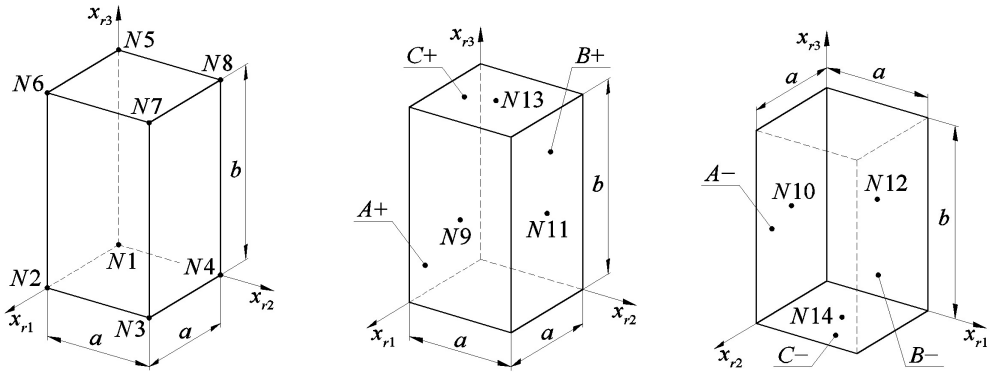

Fig. 7. Numbering of nodes in eight vertices and at the center of the sides of the roving model cell

Displacement vector of a node in the coordinate system of principal axes $x_{r1}x_{r2}x_{r3}$ of the model cell:

$$\vec{u} = u\,\vec{e}_{r1} + v\,\vec{e}_{r2} + w\,\vec{e}_{r3}. \tag{2}$$

The geometric model of the roving model cell (Fig. 5) has three orthogonal

planes of symmetry that are parallel to the sides. Because of this, the sides have special strain and periodic properties. Periodic boundary conditions are specified for the model cell due to symmetry. It ensures periodicity even if the finite element mesh is not symmetric.

The average normal strains $\bar{\varepsilon}_{r1}$, $\bar{\varepsilon}_{r2}$, $\bar{\varepsilon}_{r3}$ in the homogenized strain vector are different from 0 in the tension (pulling) simulations. The average normal stress $\bar{\sigma}_{r1}$ in the homogenized stress vector is different from zero for tension in direction x_{r1}.

The sides remain flat and move parallel due to their symmetrical properties. In order to do this the nodes are connected on the sides perpendicular to the surface:

$$u_{A-} = u(0; x_{r2}; x_{r3}) = u_{N1}, \qquad u_{A+} = u(a; x_{r2}; x_{r3}) = u_{N2}, \tag{3}$$

$$v_{B-} = v(x_{r1}; 0; x_{r3}) = v_{N5}, \qquad v_{B+} = v(x_{r1}; a; x_{r3}) = v_{N8}, \tag{4}$$

$$w_{C-} = w(x_{r1}; x_{r2}; 0) = w_{N3}, \qquad w_{C+} = w(x_{r1}; x_{r2}; b) = w_{N7}. \tag{5}$$

In formulas (3)-(5):

$$0 \le x_{r1} \le a, \qquad 0 \le x_{r2} \le a, \qquad 0 \le x_{r3} \le b. \tag{6}$$

The periodicity for the three opposite sides in all three directions are prescribed in a new way in my dissertation. The opposite nodes in the given directions on the sides are connected separately without the edges and at the edges excluded the vertices. It prevents duplication of the coordinates of the displacemnet of the nodes on certain edges and vertices, that is overdetermination. The pairs of nodes have be connected as follows:

$$A-/A+:\ v(0; x_{r2}; x_{r3}) = v(a; x_{r2}; x_{r3}),\quad w(0; x_{r2}; x_{r3}) = w(a; x_{r2}; x_{r3}), \tag{7}$$

$$B-/B+:\ u(x_{r1}; 0; x_{r3}) = u(x_{r1}; a; x_{r3}),\quad w(x_{r1}; 0; x_{r3}) = w(x_{r1}; a; x_{r3}), \tag{8}$$

$$C-/C+:\ u(x_{r1}; x_{r2}; 0) = u(x_{r1}; x_{r2}; b),\quad v(x_{r1}; x_{r2}; 0) = v(x_{r1}; x_{r2}; b). \tag{9}$$

Edges

- in direction x_{r1}: $u(x_{r1}; 0; 0) = u(x_{r1}; a; 0) = u(x_{r1}; a; b) = u(x_{r1}; 0; b)$, (10)
- in direction x_{r2}: $v(0; x_{r2}; 0) = v(0; x_{r2}; b) = v(a; x_{r2}; b) = v(a; x_{r2}; 0)$, (11)
- in direction x_{r3}: $w(0; 0; x_{r3}) = w(a; 0; x_{r3}) = w(a; a; x_{r3}) = w(0; a; x_{r3})$. (12)

In relations (7)-(12):

$$0 < x_{r1} < a, \qquad 0 < x_{r2} < a, \qquad 0 < x_{r3} < b. \tag{13}$$

In order to prevent the rigid-body like motion of the roving model cell, sides

A–, *B*– and *C*– are fixed at the nodes in the center in the direction perendicular to the surface in the case of modeling of the tension experiments:

$$u_{A-} = u_{N10} = 0\,, \qquad v_{B-} = v_{N12} = 0\,, \qquad w_{C-} = w_{N14} = 0\,. \tag{14}$$

$\bar{\varepsilon}_{r1}$ is given in the case of uniaxial tension in direction x_{r1}. Displacement u_{A+} (of side *A*+) follows from it as kinematic load:

$$u_{A+} = u_{N9} = a\,\bar{\varepsilon}_{r1}\,. \tag{15}$$

Cross contractions (displacements in plane perpendicular to the direction of tension) and reaction forces numerically deteremined with finite element roving model cell in the case of tension in direction x_{r1} are as follows:

$$\begin{aligned} &v_{B+}\,,\ w_{C+}\,,\\ &\vec{F}_{rA+} = F_{r1A+}\vec{e}_{r1}, \qquad \vec{F}_{rA-} = F_{r1A-}\vec{e}_{r1}, \qquad \left(\vec{F}_{rA+} = -\vec{F}_{rA-}\right),\\ &\vec{F}_{rB-} = \vec{F}_{rC-} = \vec{0}\,. \end{aligned} \tag{16}$$

The reaction force is reduced into the central node because every node is connected on the sides in the direction of clamping and load according to equations (3)-(5).

It is a new idea that the average stress is calculated as the quotient of the reaction force occuring on the sides and the original area of the surface of the side. The average normal stress $\bar{\sigma}_{r1}$ is determined in the same way. Young's modulus of the roving in direction x_{r1} can be calculated in the usual way:

$$\bar{\sigma}_{r1} = \frac{1}{A_{A+}} \int\limits_{(A_{A+})} \sigma_{r1}\,dA = \frac{F_{r1A+}}{A_{A+}}, \tag{17}$$

$$E_{r1} = \frac{\bar{\sigma}_{r1}}{\bar{\varepsilon}_{r1}}. \tag{18}$$

Poisson's ratio is the ratio of the transverse and longitudinal strains at the uniaxial stress state. Poisson's ratios of homogenised material can be obtained from appropriate data of the calculated displacement field:

$$\nu_{r12} = -\frac{\bar{\varepsilon}_{r2}}{\bar{\varepsilon}_{r1}} = -\frac{v_{B+}}{a}\frac{a}{u_{A+}} = -\frac{v_{B+}}{u_{A+}}, \quad \nu_{r13} = -\frac{\bar{\varepsilon}_{r3}}{\bar{\varepsilon}_{r1}} = -\frac{w_{C+}}{b}\frac{a}{u_{A+}} = -\frac{w_{C+}}{u_{A+}}\frac{a}{b}. \tag{19}$$

2.3. Finite element model cell of the textile composit layer

A textile composite layer is made of domains repeating in the directions of warp and weft. The layer model cell is a repeating part of the layer from which the composite layer can be built. Parametric dimensions of model cell of a composite layer reinforced by plain weave textile are shown in Fig. 8. It shows also the numbering of the six sides. Dimensions of layer model cell built on one of the layers of eight-layer, plain weave textile, composite sheet of Fig. 2 are as follows:

$$a = b = 4 \text{ mm}, \; h = 0{,}25 \text{ mm}, \; t_1 = t_2 = 2 \text{ mm}, \; s_{r1} = s_{r2} = 1{,}8 \text{ mm},$$
$$A_{A+} = A_{A-} = 1 \text{ mm}^2, \; A_{B+} = A_{B-} = 1 \text{ mm}^2, \; A_{C+} = A_{C-} = 16 \text{ mm}^2.$$

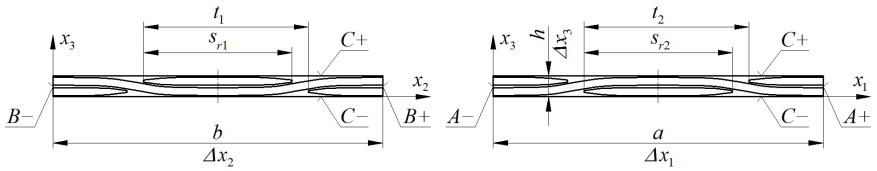

Fig. 8. Geometry and dimensions of the layer model cell

Sides of the model cell perpendicular to axes x_1 and x_2 are set so that they contain one symmetric unit in the direction of warp and one symmetric unit in the direction of weft (Fig. 8). The sides coincide with the planes of principal axes $x_{r1}x_{r3}$ and $x_{r2}x_{r3}$ (Fig. 9).

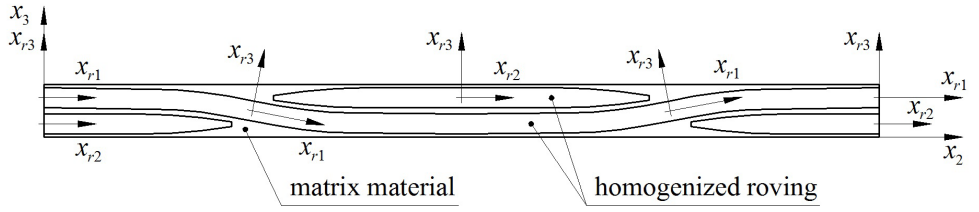

Fig. 9. Coordinate system $x_1x_2x_3$ of the layer model cell and principal axes x_{r1}, x_{r2}, x_{r3} of rovings

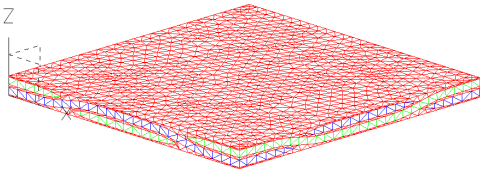

Fig. 10. Finite element mesh of the layer model cell

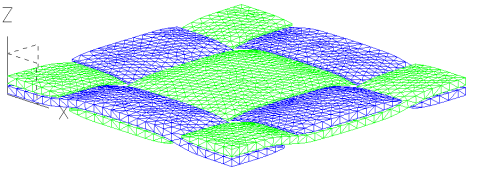

Fig. 11. Finite element mesh of the textile layer

Finite element mesh of the layer model cell is shown in Fig. 10. Finite element mesh of the textile layer can be seen in Fig. 11. The nodes facing

each other on the three sides of the model cell are at the same coordinates. Coordinate system XYZ is the coordinate system of the principal axes $x_1x_2x_3$ of the layer model cell.

There are four independent macroscopic material constants in planar orthotropic Hooke's law of textile composite layer: E_1, E_2, ν_{12}, G_{12}. Table 3 shows which material constant can be determined in a given load case. Since the reinforcement is the same in the longitudinal and transverse directions for the model cell studied, Young's modulus and the Poisson's ratio of the reinforced composite layer (of the whole composite sheet in the case of the same layer structure) are the same in directions x_1 and x_2:

$$E_1 = E_2, \qquad \nu_{12} = \nu_{21}. \tag{20}$$

Table 3. Characteristic material constants of the composite layer

Simulated load cases	Determinable material constants	Check
Tension in direction x_1	E_1, ν_{12}	$\frac{\nu_{12}}{E_1} = \frac{\nu_{21}}{E_2}$, $\nu_{21} = \frac{E_2}{E_1}\nu_{12}$
Tension in direction x_2	E_2, ν_{21}	
Shear in plane x_1x_2	G_{12}	

Every load case in Table 3 is simulated with layer model cell. Shear in plane x_1x_2 is presented in the booklet of thesis.

Kinematic load (a nodal displacement field) is specified for the layer model cell of textile composite, too. Numbers shown in Fig. 12 refer to the nodes in the vertices and at the center of the sides of the model cell.

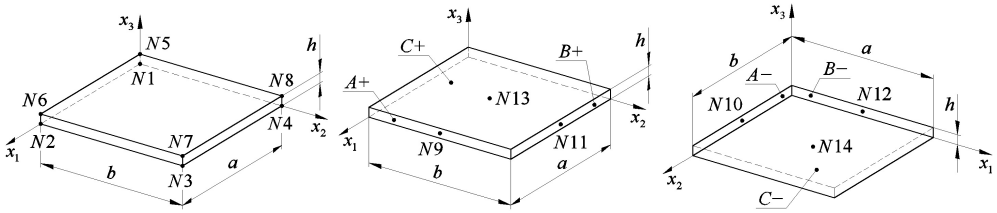

Fig. 12. Numbering of nodes in eight vertices and at the center of the sides of the layer model cell

Displacement vector of a node in the coordinate system of principal axes $x_1x_2x_3$ of the model cell:

$$\vec{u} = u\,\vec{e}_1 + v\,\vec{e}_2 + w\,\vec{e}_3. \tag{21}$$

Pure shear in plane x_1x_2 has to be simulated for determination of shear modulus G_{12} of the textile composite layer. The average strains in both

directions must be zero in this case. Only average shear strain $\overline{\gamma}_{12}$ in the average strain vector is not zero. It must be required in the simulation:

$$\overline{\gamma}_{12} = \frac{1}{2}\overline{\gamma}_{12} + \frac{1}{2}\overline{\gamma}_{21}, \qquad \frac{1}{2}\overline{\gamma}_{12} = \frac{1}{2}\overline{\gamma}_{21}. \tag{22}$$

Average shear stress $\overline{\tau}_{12}$ in homogenized stress vector is different from zero.

There is a plane of symmetry of the layer model cell which is perpendicular to axes x_1 and x_2 (Fig. 8). Sides *A*–, *A*+, *B*– and *B*+ are planes of symmetry of periodically adjacent model cells. Because of this there is no strain in direction x_2 on sides perpendicular to axis x_1 and in direction x_1 on sides perpendicular to axis x_2 in the case of shear in plane x_1x_2. It is achieved by connecting rigidly all nodes on the sides according to the follows:

$$v_{A-} = v(0; x_2; x_3) = v_{N1}, \qquad v_{A+} = v(a; x_2; x_3) = v_{N2}, \tag{23}$$

$$u_{B-} = u(x_1; 0; x_3) = u_{N5}, \qquad u_{B+} = u(x_1; b; x_3) = u_{N8}. \tag{24}$$

In equations (23) and (24):

$$0 \le x_1 \le a, \qquad 0 \le x_2 \le b, \qquad 0 \le x_3 \le h. \tag{25}$$

The pure shear is modeled by prescribed displacement in direction x_2 of sides perpendicular to axis x_1 and prescribed displacement in direction x_1 of sides perpendicular to axis x_2. Kinematic prescriptions needed for this are specified at the nodes in the center of the sides *A*+, *A*–, *B*+, *B*–:

$$v_{A-} = v_{N10} = 0, \qquad v_{A+} = v_{N9} = a\frac{1}{2}\overline{\gamma}_{21}, \tag{26}$$

$$u_{B-} = u_{N12} = 0, \qquad u_{B+} = u_{N11} = b\frac{1}{2}\overline{\gamma}_{12}. \tag{27}$$

In order to prevent the rigid-body like motion, node *N1* in the origin is not allowed to move in direction x_3:

$$w_{N1} = 0. \tag{28}$$

New method also for the layer model cell is that the opposite nodes in the given directions on the sides are connected separately without the edges and at the edges excluded the vertices. The pairs of the nodes must be connected according to (29)-(38) for ensuring the periodicity in the case of shear. The way the nodes above each other on sides $C-/C+$ are connected is also a new method.

$$A-/A+:\ u(0;x_2;x_3)=u(a;x_2;x_3),\qquad w(0;x_2;x_3)=w(a;x_2;x_3), \tag{29}$$

$$B-/B+:\ v(x_1;0;x_3)=v(x_1;b;x_3),\qquad w(x_1;0;x_3)=w(x_1;b;x_3), \tag{30}$$

$$C-/C+:\ u(x_1;x_2;0)=u(x_1;x_2;h),\qquad v(x_1;x_2;0)=v(x_1;x_2;h). \tag{31}$$

Edges

- in direction x_1:

$$v(x_1;0;0)=v(x_1;b;0),\quad w(x_1;0;0)=w(x_1;b;0), \tag{32}$$

$$v(x_1;0;h)=v(x_1;b;h),\quad w(x_1;0;h)=w(x_1;b;h), \tag{33}$$

$$v(x_1;b;0)=v(x_1;b;h). \tag{34}$$

- in direction x_2:

$$u(0;x_2;0)=u(a;x_2;0),\ w(0;x_2;0)=w(a;x_2;0), \tag{35}$$

$$u(0;x_2;h)=u(a;x_2;h),\ w(0;x_2;h)=w(a;x_2;h), \tag{36}$$

$$u(a;x_2;0)=u(a;x_2;h). \tag{37}$$

- in direction x_3:

$$w(0;0;x_3)=w(a;0;x_3)=w(a;b;x_3)=w(0;b;x_3). \tag{38}$$

In equations (29)-(38):

$$0<x_1<a,\qquad 0<x_2<b,\qquad 0<x_3<h. \tag{39}$$

Nodes in vertices are connected in direction x_3 on sides *C*– and *C*+:

$$w_{N1}=w_{N2}=w_{N4}=w_{N3},\qquad w_{N5}=w_{N6}=w_{N8}=w_{N7}. \tag{40}$$

Reaction forces determined by finite element calculation in the case of shear in plane x_1x_2:

$$\begin{aligned}
&\vec{F}_{A+}=F_{2A+}\vec{e}_2,\qquad \vec{F}_{A-}=F_{2A-}\vec{e}_2,\qquad \left(\vec{F}_{A+}=-\vec{F}_{A-}\right),\\
&\vec{F}_{B+}=F_{1B+}\vec{e}_1,\qquad \vec{F}_{B-}=F_{1B-}\vec{e}_1,\qquad \left(\vec{F}_{B+}=-\vec{F}_{B-}\right),\\
&\vec{F}_{N1}=\vec{0}.
\end{aligned} \tag{41}$$

The average shear stresses (which are the same because of the duality of stresses τ) are determined by quotient of reaction force and original area of side similarly to equation (17):

$$\overline{\tau}_{12}=\frac{F_{1B+}}{A_{B+}},\qquad \overline{\tau}_{21}=\frac{F_{2A+}}{A_{A+}}. \tag{42}$$

Shear modulus of the textile composite layer in plane x_1x_2:

$$G_{12}=\frac{\overline{\tau}_{12}}{\overline{\gamma}_{12}}. \tag{43}$$

3. RESULTS

Macroscopic material properties determined by the model cell of the textile composite sheet will be desribed cell in this chapter. Material properties obtained by the model cells are compared with the measurement results. It validates the applicability of roving and textile composite layer model cells in engineering calculations. Also parameter studies were carried out with model cells. The change of mechanical properties of a textile composite layer was analyzed. It will be presented what factors were studied.

3.1. Prescribed macroscopic material properties of roving

Table 4 summaries the following quantities in the case of tension in the direction x_{r1} presented in Chapter 2.2: prescribed kinematic load, quantities determined numerically, and the derived average stress and material properties.

Table 4. Prescribed and determined quantities in the case of tension in the direction x_{r1}

Kinematic load	$\bar{\varepsilon}_{r1} = 2{,}5 \cdot 10^{-3}$, $u_{A+} = u_{N9} = 19{,}0325 \cdot 10^{-3}$ µm
Quantities determined by finite element method	$v_{B+} = -3{,}854 \cdot 10^{-3}$ µm, $w_{C+} = -6{,}675 \cdot 10^{-3}$ µm
	$\vec{F}_{rA+} = (44\,479{,}2\vec{e}_{r1})$ µN, $\vec{F}_{rA-} = (-44\,479{,}2\vec{e}_{r1})$ µN
Average stress	$\bar{\sigma}_{r1} = 443{,}09$ MPa
Material constants	$E_{r1} = 177\,236$ MPa, $\nu_{r12} = 0{,}202$, $\nu_{r13} = 0{,}202$

The roving model cell is linear elastic. Table 5 contains twelve material constants which were determined by finite element roving model cell with six load cases described in Table 2. The roving is orthotropic and it is isotropic in transverse direction.

Table 5. Material constants determined by roving model cell

$E_{r1} = 177\,236$ MPa	$E_{r2} = 10\,352$ MPa	$E_{r3} = 10\,352$ MPa
$\nu_{r12} = 0{,}202$	$\nu_{r21} = 0{,}012$	$\nu_{r31} = 0{,}012$
$\nu_{r13} = 0{,}202$	$\nu_{r23} = 0{,}430$	$\nu_{r32} = 0{,}430$
$G_{r12} = 4\,115$ MPa	$G_{r23} = 3\,620$ MPa	$G_{r13} = 4\,115$ MPa

3.2. Determined macroscopic material properties of composite layer

Table 6 contains the following quantities: prescribed kinematic loads presented in Chapter 2.3 in the case of pure shear in plane x_1x_2, reaction

forces determined by finite element method, derived average shear stresses and shear modulus.

Table 6. Prescribed and determined quantities in the case of shear in plane x_1x_2

Kinematic load	$\overline{\gamma}_{12} = 2 \cdot 10^{-3}$, $\frac{1}{2}\overline{\gamma}_{12} = \frac{1}{2}\overline{\gamma}_{21} = 10^{-3}$
	$v_{A+} = v_{N9} = 4 \cdot 10^{-3}$ mm , $u_{B+} = u_{N11} = 4 \cdot 10^{-3}$ mm
Reaction forces	$\vec{F}_{A+} = (5{,}8\vec{e}_2)$ N , $\vec{F}_{A-} = (-5{,}8\vec{e}_2)$ N
	$\vec{F}_{B+} = (5{,}8\vec{e}_1)$ N , $\vec{F}_{B-} = (-5{,}8\vec{e}_1)$ N
Averaged stress	$\overline{\tau}_{12} = 5{,}8$ MPa , $\overline{\tau}_{21} = 5{,}8$ MPa
Shear modulus	$G_{12} = 2\,900$ MPa

Eight-layer textile composite sheet in Fig. 2 is linear elastic and orthotropic. Table 7 contains its macroscopic material properties determined by finite element layer model cell. The five orthotropic material constants are calculated with three load cases presented in Table 3.

Table 7. Material constants determined by model cell of composite layer

$E_1 = 50\,720$ MPa	$E_2 = 50\,720$ MPa
$\nu_{12} = 0{,}103$	$\nu_{21} = 0{,}103$
$G_{12} = 2\,900$ MPa	

3.3. Applicability of finite element model cells

The roving model cell was developed for the case where the fibers in the roving are untwisted and parallel to each other. Further numerical examination is required for twisted rovings.

It is required for textile composite layer model cell that the reinforcing fabric be flat, 2D. Rovings in the textile have to run in two directions, which are perpendicular to each other. Also the macroscopic orthotropic material properties of a one direction reinforced composite layer can be determined using the layer model cell shown. The applicability of the method does not depend on the material properties of the roving and the matrix, the cross section, width, spacing of the rovings, and the weave pattern of the textile. In order to use the boundary conditions shown in the layer model cell, it is a condition that the sides of the model cell coincide with the planes of the material principal directions of the rovings, as in Fig. 9. There must be no side at the junction. It is not necessary that the structure of the textile and the periodic part modeled are symmetrical for the application of boundary

conditions. So my model cell can be extended to a non-symmetric case.

3.4. Validation of finite element model cell for roving and textile composite layer

The finite element model cell of roving and textile composite layer and the developed modeling method have been validated by comparing the material properties obtained with the layer model cell with the measurement results.

The finite element model cell is also orthotropic, linear like in the case of experiments of tension and shear of the textile composite sheet. Table 8 contains: material constants of the textile composite layer E_1, E_2, ν_{12}, ν_{21} and G_{12} determined by measurements, as well as the minimum and maximum values belonging to the margin of error. Table 9 summarizes the macroscopic orthotropic material properties determined by finite element model cells, as well as the deviation of results of layer model cell from the mean values of measurement.

Table 8. Material constants of textile composite layer determined by measurements

Material constants determined by measurements	Minimum	Maximum
$E_1 = E_2 = 50\,094 \pm 1\,480$ MPa	$E_1 = E_2 = 48\,614$ MPa	$E_1 = E_2 = 51\,574$ MPa
$\nu_{12} = \nu_{21} = 0{,}102 \pm 0{,}016$	$\nu_{12} = \nu_{21} = 0{,}086$	$\nu_{12} = \nu_{21} = 0{,}118$
$G_{12} = 3\,018 \pm 254$ MPa	$G_{12} = 2\,764$ MPa	$G_{12} = 3\,272$ MPa

Table 9. Comparison of results of roving and layer model cell with measurement results

Material constants determined by model cell of textile composite layer	Deviation of the result of the model cell from the mean value of the measurement	
$E_1 = E_2 = 50\,720$ MPa	+626 MPa	+1,25 %
$\nu_{12} = \nu_{21} = 0{,}103$	+0,001	+0,98 %
$G_{12} = 2\,900$ MPa	−118 MPa	−3,91 %

It can be stated that the results and material properties of the textile composite layer with finite element roving and layer model cell are within the margin of error of measurement and the deviation is below 4% compared to the average of the measurement. This proves that the results of the finite element model cell of the roving and the textile composite layer reach the required accuracy for engineering modeling and engineering calculations.

3.5. Creating required composite layer material properties

Four parameter tests were performed to analyze the change of mechanical properties of a composite layer. The results of the parametric investigations are summarized in Chapter 4 (New scientific results).

The thickness of the layer is the same in each layer model cell. The rovings have the same geometry as the Torayca T300-3K in each case (Fig. 3), except that the material properties differ only in the parameter study of the effect of Young's modulus of the reinforcing fiber on the layer material properties. In all cases, the matrix material is AROPOL M105TB polyester resin whose isotropic material properties shown in Table 1.

Effect of Young's modulus of the reinforcing fiber

The material properties of the textile composite layer are investigated with respect to the Young's modulus of the fiber by keeping the ratio of the transverse and longitudinal modulus of the fiber constant:

$$\delta = \frac{E_{f2}}{E_{f1}} = 0{,}08\,. \tag{44}$$

The values used in the model cell validation, which are shown in Table 1, are used for three independent material constants ν_{f12}, ν_{f23}, G_{f12}. The carbon fiber is assumed to be isotropic in the transverse direction, so by changing Young's modulus E_{f2} shear modulus G_{f23} is also changed. Shear modulus G_{f23} is calculated as a function of E_{f2} and ν_{f23}:

$$G_{f23} = \frac{E_{f2}}{2\left(1+\nu_{f23}\right)}. \tag{45}$$

Three parameter variants are studied:

a) $E_{f1} = 200\,000$ MPa, $E_{f2} = 16\,000$ MPa,

b) $E_{f1} = 225\,000$ MPa, $E_{f2} = 18\,000$ MPa,

c) $E_{f1} = 250\,000$ MPa, $E_{f2} = 20\,000$ MPa.

Model cells shown in sections 2.2, 2.3 are used for the test. Macroscopic roving material properties are determined for three carbon fiber material properties with finite element roving model cell. These are then given to the material properties of the homogenized roving for the textile composite layer model cell.

Changes of layer material properties in the case of different weave patterns

The material constants of textile composite layer are investigated. How are they changed when a roving crosses several successive perpendicular rovings at the bottom or top, making a roving less wavy over a given length. 4 different textile reinforced layers are modeled. There are not over and under crossings in knitted biaxial fabric. Reinforcements tested:

a) 1×1 that is plain weave textile,
b) 2×2 basket weave textile,
c) 3×3 basket weave textile and
d) knitted biaxial fabric.

Effect of the ratio of volume of the textile on material properties of the layer

Volume ratio of the elementary fibers φ_f in composite layers are changed by spacing t_1, t_2 of rovings shown in Fig. 8. Three cases below are studied:

a) $t_1 = t_2 = 3$ mm, $\varphi_f = 0{,}307$,
b) $t_1 = t_2 = 2{,}5$ mm, $\varphi_f = 0{,}368$,
c) $t_1 = t_2 = 2$ mm, $\varphi_f = 0{,}461$.

Effect of the ratio of longitudinal to transverse rovings

It is investigated how the orthotropic material properties of the textile composite layer change by changing the ratio of longitudinal and transverse fiber bundles in the textile. The distance of longitudinal rovings is the same in every layer model cell: $t_1 = 2$ mm. Distance of the transverse rovings t_2 differs in each model. Ratio of longitudinal to transverse rovings λ can be expressed by distance of rovings t_i and density of rovings n_i $(i = 1, 2)$:

$$\lambda = \frac{n_2}{n_1} = \frac{t_1}{t_2}. \tag{46}$$

Properties of five layer model cells studied:

a) There is no transverse roving: $n_2 = 0$, $(t_2 = \infty)$, $\lambda = 0$,
b) $t_2 = 4$ mm, $\lambda = 0{,}5$,
c) $t_2 = 3$ mm, $\lambda = 0{,}67$,
d) $t_2 = 2{,}5$ mm, $\lambda = 0{,}8$,
e) $t_2 = 2$ mm, $\lambda = 1$.

4. NEW SCIENTIFIC RESULTS

1. Finite element model cell of untwisted roving

Based on literature sources, a finite element roving model cell has been developed to determine numerically the material constants of an untwisted roving made of thousands of elementary fibers impregnated with matrix material. Macroscopic material properties of a homogeneous orthotropic roving E_{r1}, E_{r2}, E_{r3}, ν_{r12}, ν_{r23}, ν_{r13}, G_{r12}, G_{r23}, G_{r13} can be determined with the model cell in principal coordinate system knowing the material properties of the elementary fibers and the matrix, and the cross section geometry of the roving. The material constants can be generated by the computer simulation I have developed. It models the axial tension in the direction of axes x_{r1}, x_{r2}, x_{r3} of the roving cell and shear in plane $x_{r1}x_{r2}$, $x_{r2}x_{r3}$, $x_{r1}x_{r3}$.

The kinematic requirements are realized in a novel way by fixed support (kinematic load) the center node of the cell side, and the stresses are determined from the reaction forces reduced to the center node. New idea is to connect the opposing nodes to each other separately on the sides and edges. It ensures the periodic behavior of the model cell on the three opposite sides in all three directions, preventing the overdetermination of nodes at edges and vertices. Such symmetry conditions are defined that are consistent with the periodic boundary conditions. Thus, the simulated load cases are not only applicable to a symmetrical finite element mesh.

2. Finite element model cell of textile composit layer

Using the literature a finite element model cell has been developed for determining numerically the material constants of a composite layer made of textile woven from rovings and impregnated with matrix material. The model cell can be used to calculate material properties E_1, E_2, ν_{12} and G_{12} of the composite layer modeled by homogeneous orthotropic material knowing the material properties of rovings and matrix, as well as the geometry of the reinforced textile and thickness of the layer. The material properties are determined by finite element model experiments for axial tension in direction x_1, x_2 and shear in plane x_1x_2. I have developed this numerical method.

The novelty of modeling is that the reaction force on the four lateral sides of the layer model cell is reduced to the central node. Fixed supports and kinematic loads are given on the central node. The nodes are connected on the side in the direction of fixed supports and loads. The stresses are

determined from reaction forces. Refinement of modeling: opposing nodes on sides, edges and vertices are connected separately in given directions. It ensures that there is no overdetermined node at edges and vertices. New is that nodes above each other in the model cell are connected in two directions in the plane of the layer. So bending due to the decrease and increase of waviness from weaving does not occur in any layer of the composite sheet.

Measurements proved that the accuracy of the material properties determined by the finite element model cell of the roving and the textile composite layer reaches the extent necessary for engineering calculations. The validation of numerical modeling by measurements confirms the usefulness of the novel modeling I applied.

3. Effect of Young's modulus of reinforcing fiber on material properties of layer

Parameter analysis carried out by finite element roving and composite layer model cells has proved that Young's modulus E_1 of the composite layer increases approximately linearly with Young's modulus E_{f1} (and E_{f2}) of the reinforcing fibers. The ratio E_1/E_{f1} decreases by reciprocal function becasue Young's modulus E_1 of the textile composite layer increases slower than Young's modulus E_{f1} of reinforcing fiber.

It is shown that Poisson's ratio of the composite layer ν_{12} increases approximately linearly with E_{f1} and E_{f2}. But changes of Young's modulus of the reinforcing fiber do not affect shear modulus G_{12} of the composite layer.

Validity range of the examination: $E_{f1} = 200 - 250$ GPa , $E_{f2} = 16 - 20$ GPa . It is assumed that the ratio of transverse Young's modulus to longitudinal Young's modulus of elementary fibers is constant, it is $\delta = E_{f2}/E_{f1} = 0{,}08$ with average values in practice.

4. Changes of material properties of layer in the case of different weaving patterns

The effect of the change of the textile weaving pattern on the material properties of the layer is determined by applying layer model cells and parameter analysis.

The parameter analysis has proved that if the number of waves resulting from the weaving is reduced within a given length in roving of the textile

(that is weave pattern is changed), Young's modulus E_1 of the composite layer is increased, and Poisson's ratio ν_{12} of the composite layer is decreased. It is found that the shear modulus G_{12} is not affected by the weave pattern.

5. Effect of volume ratio of textile on material properties of the composite layer

It has shown using layer model cells and parameter analysis how the volume ratio φ_f of textil affects the material properties of the composite layer. The widths s_r of the rovings and the thickness *h* of the composite layer are kept constant during the test, and the volume ratio is changed by the distance *t* of the rovings. The examined $\varphi_f = 0{,}301-0{,}461$ range is determined by the weaving technology feasibility at $s_r/t = 0{,}6-0{,}9$ ratio.

It is found that Young's modulus E_1, Poisson's ratio ν_{12} and shear modulus G_{12} also increase with the volume ratio of the textile. G_{12} increases almost linearly.

6. Effect of ratio of longitudinal to transverse rovings in the textile on material properties of the layer

The effect of the ratio λ of the longitudinal and transverse rovings on the material properties of the composite layer is determined using layer model cells. The width of the rovings in the textile is constant and the same in both directions during the test: $s_{r1} = s_{r2}$. Ratio $\lambda = t_1/t_2$ is modified such way that distance t_1 of rovings in direction x_1, ratio $s_{r1}/t_1 = 0{,}9$ are not changed but distance t_2 of rovings in direction x_2, ratio s_{r2}/t_2 are changed. The numerical simulation is carried out taking into account the textile types that occur in practice: $\lambda = 0$ $(s_{r2}/t_2 = 0)$, $\lambda = 0{,}5-1$ $(s_{r2}/t_2 = 0{,}45-0{,}9)$. In the case of $\lambda = 0$ there is not transverse roving. It is the unidirectional fiber reinforcing.

It has been shown that the longitudinal Young's E_1 modulus has a local maximum when changing the fiber ratio λ. When the longitudinal rovings reach a given waviness, the textile composite layer loses part of its rigidity in direction x_1. Numerical analysis has proved that transverse Young's modulus E_2 is approximately linear function of λ. Poisson's ratio ν_{12} (cross

contraction in the case of tension in direction x_1) has maximum at $\lambda = 0$. ν_{12} decreases as a function of the ratio of longitudinal and transverse rovings, and then increases slightly after a local minimum. ν_{21} is a monotone increasing function of λ. If the composite layer is reinforced in direction x_2 and thus there are several waves in the rovings in direction x_1 within a given length, the cross contraction increases in the case of tension in direction x_2. Shear modulus G_{12} increases approximately linearly as a function of the ratio of longitudinal to transverse rovings.

5. CONCLUSIONS AND SUGGESTIONS

Composite layered structures are modeled with layered composite shell elements in finite element program systems. For these elements, the input data must specify the thickness for each layer, the orientation angle of the principal direction x_1 and the four independent material constants in the coordinate system of principal directions x_1x_2: E_1, E_2, ν_{12}, (ν_{21}) and G_{12}. Several methods have recently been published to determine the material properties of a composite layer using the finite element method.

The finite element model cell of the textile composite layer, which I have developed and improved, determines numerically the macroscopic orthotropic material properties of a layer, by knowing the matrix and roving material properties, as well as the geometry of the reinforcement textile structure and the thickness of the layer. The rovings should be modeled not with elementary fibers but with a homogeneous orthotropic material in a layer model cell.

The finite element roving model cell I built and improved can be used to obtain the macroscopic orthotropic material properties of a matrix impregnated roving containing thousands of elementary fibers.

With the two tools above (finite element roving model cell and finite element layer model cell), it is possible to determine the macroscopic material properties of a composite layer with the precision needed for engineering modeling without producing specimens.

A layer may be expected to have some required mechanical properties for layered composite structures. Therefore I performed parameter investigations on how the following factors influence the macroscopic material properties of a layer:

– changes of Young's modulus of the reinforcing fiber,
– changes of weave pattern of the textile,
– changes of the ratio of the volume of the reinforcing textile,
– changes of the ratio of longitudinal to transverse rovings in the textile.

These parameter tests provide a good starting point, estimation, by which the material properties of a textile composite layer can be adjusted according to the specifications and expectations.

With the model cells developed in my PhD thesis not only material properties of textile composite layer but also macroscopic material properties of unidirectionally reinforced composite layer can be produced.

6. SUMMARY

The aim of this dissertation is to develop finite element model cells for determination of macroscopic material constants of rovings and textile composite layers made from these rovings. In the elaboration I have taken into consideration and developed the finite element models described in the literature.

I made eight-layer tensile and shear specimens from a given textile and matrix material. Experimental investigation was carried out to determine the macroscopic material properties of the orthotropic composite sheet, which are identical to the material properties of a composite layer. I also produced specimens from the matrix material and determined the isotropic material properties of the matrix.

Roving finite element model cell was developed for the textile roving (embedded in the matrix) of textile composite test specimen used in experiments. The model cell was used to perform finite element analysis and to produce macroscopic orthotropic material properties of the roving.

Then I developed a finite element layer model cell for one layer of the textile composite specimen used in the experiments. The material properties determined by the roving model cell were used for a roving of the textile material. The layer model cell was used to produce the planar macroscopic material properties of the layer.

The edges were excluded at specifying the periodic boundary conditions of the opposing sides, and the vertices were excluded at specifying the periodic boundaries of the opposite edges in the model cells, in order to avoid the overdetermination of the nodes. Kinematic load, nodal displacement field were prescribed. The average stress in the model cells was calculated from the reaction forces on the sides.

I checked the roving and layer model cell by comparing the numerical results of the measurement and the finite element model cells. The material properties determined by the model cells are within the margin of error of measurements, and the deviation is less than 4% of the mean of the measurement. This comparison demonstrates the applicability of finite element textile roving and textile composite layer model cells in engineering calculations.

Further aim of my research was to investigate the effect of certain parameters on the macroscopic orthotropic material properties of textile composite layer with finite element model cells. I examined the change of Young's modulus of the reinforcing fiber in the textile roving. I analyzed the change of the weave pattern, volume ratio and ratio of the longitudinal to transverse roving of the reinforcing textile. I drew diagrams that give guidance on how certain factors influence the orthotropic material properties of the composite layer.

7. MOST IMPORTANT PUBLICATIONS RELATED TO THE THESIS

Referred articles in foreign languages

1. **Bojtár, G.**; M. Csizmadia, B.; Égert, J. (2016): Numerical estimation method of orthotropic material properties of a roving for reinforcement of composite materials. Acta Polytechnica Hungarica, Vol. 13, No. 6, pp. 163-182., ISSN 1785-8860, (IF: 0,745)
2. **Bojtár, G.**; M. Csizmadia, B.; Égert, J. (2017): Numerical determination of orthotropic material properties of textile composite layers and their validation by measurement. Acta Polytechnica Hungarica, Vol. 14, No. 2, pp. 47-67., ISSN 1785-8860, (IF: 0,909)

Referred articles in Hungarian

3. **Bojtár G.**, M. Csizmadia B., Égert J. (2008): Üvegszálas textil kompozit anyagok mechanikai viselkedésének végeselemes modellezése. GÉP, LIX. évf., 10-11. sz., 23-29. o., ISSN 0016-8572
4. **Bojtár G.**, Égert J. (2009): 2D és 3D végeselem modellcellák textil-kompozit rétegek anyagállandóinak meghatározására. EMT Műszaki Szemle, Különszám 2009, XVII. OGÉT 2009., 69-74. o., ISSN 1454-0746
5. Aczél Á., **Bojtár G.**, Fehér L., Keresztes D. (2011): Versenyautó alváz térbeli rúdmodelljének végeselemes analízise. GÉP, LXII. évf., 7-8. sz., 3-8. o., ISSN 0016-8572